Histological study on regional specificity of the mucosal nerve network in the rat large intestine

Nakanishi, Satoki ; Mantani, Youhei ; Ohno, Nobuhiko ; Morishita, Rinako ; Yokoyama, Toshifumi ; Hoshi, Nobuhiko

(Citation)
Journal of Veterinary Medical Science,85(2):123-134

(Issue Date)
2023-02

(Resource Type)
journal article

(Version)
Version of Record

(URL)
https://hdl.handle.net/20.500.14094/0100482620

The Journal of Veterinary Medical Science

FULL PAPER

Anatomy

Histological study on regional specificity of the mucosal nerve network in the rat large intestine

Satoki NAKANISHI[1)], Youhei MANTANI[1)]*, Nobuhiko OHNO[3,4)], Rinako MORISHITA[1)], Toshifumi YOKOYAMA[2)], Nobuhiko HOSHI[2)]

[1)]Laboratory of Histophysiology, Department of Bioresource Science, Graduate School of Agricultural Science, Kobe University, Hyogo, Japan
[2)]Laboratory of Animal Molecular Morphology, Department of Bioresource Science, Graduate School of Agricultural Science, Kobe University, Hyogo, Japan
[3)]Department of Anatomy, Division of Histology and Cell Biology, Jichi Medical University, School of Medicine, Tochigi, Japan
[4)]Division of Ultrastructural Research, National Institute for Physiological Sciences, Aichi, Japan

ABSTRACT. Our previous studies and others have revealed detailed characteristics of the mucosal nerve network in the small intestine, but much remains unknown about the corresponding network in the large intestine. We herein investigated regional differences in the expression of neurochemical markers, the nerve network structure, and the cells in contact with nerve fibers by histological analysis using both immunohistochemistry and serial block-face scanning electron microscopy (SBF-SEM). Immunohistochemistry revealed that immunopositive structures for protein gene product 9.5, vasoactive intestinal peptide (VIP), calretinin and vesicular acetylcholine transporter were more prevalent in the lamina propria of the ascending colon than the cecum and descending colon (DC). There was no significant difference in the frequency of most neurochemical markers between the cecum and DC, but the frequencies of VIP^+ structures were higher in the cecum than in the DC. SBF-SEM analysis showed that the nerve network structure was more developed on the luminal side of the DC than the cecum. The cells that nerve fibers abundantly contacted were subepithelial and lamina propria fibroblast-like cells and macrophages. In addition, nerve fibers in the cecum were in more frequent contact with immune cells such as macrophages and plasma cells than nerve fibers in the DC. Thus, the present histological analysis suggested that the mucosal nerve network in the large intestine possessed both regional universality and various specificities, and revealed the intimate relationship between the nerve network and immune cells, especially in the cecum.

KEYWORDS: electron microscopy, enteric nervous system, immunohistochemistry, large intestine, nerve fiber

J. Vet. Med. Sci.
85(2): 123–134, 2023
doi: 10.1292/jvms.22-0433

Received: 12 September 2022
Accepted: 27 November 2022
Advanced Epub:
13 December 2022

The enteric nervous system is a highly developed nervous system in the gastrointestinal tract, and is known to play regulatory roles in activities such as blood flow, the secretion of intestinal juice and the movement in the intestine [16]. The mucosal nerve network of the small intestine has been investigated using immunohistochemistry and other experimental techniques. Neurons in the submucosal plexus of the mouse small intestine, which abundantly innervate the mucosa, have been classified by immunohistochemistry, based on the expression of various neurochemical markers such as calcitonin gene-related peptide (CGRP), choline acetyltransferase, calretinin (CR), substance P (SP) vasoactive intestinal peptide (VIP), and others [42, 48]. In fact, cholecystokinin (CCK), CGRP, neuropeptide Y (NPY), SP, somatostatin (SST), tyrosine hydroxylase, vesicular acetylcholine transporter (VAChT), or VIP immunopositive nerve fibers are present in the mucosa of mouse and/or guinea pig small intestine [30, 36, 42]. In addition, NPY^+ neurons co-positive for CGRP, CCK, choline acetyltransferase, or SST in the submucosal plexus extend nerve fibers into the mucosa [17, 18]. On the other hand, studies using transmission electron microscopy have revealed that nerve fibers are in contact with fibroblast-like cells [11, 24, 44], mononuclear phagocytes [8] and mast cells [52] in the rat or mouse small intestine. Furthermore, in our previous study we used serial block-face scanning electron microscopy (SBF-SEM), a type of volume electron microscopy, to three-dimensionally analyze

*Correspondence to: Mantani Y: mantani@sapphire.kobe-u.ac.jp, Laboratory of Histophysiology, Graduate School of Agricultural Science, Kobe University, 1-1 Rokkodai-cho, Nada-ku, Kobe, Hyogo 657-8501, Japan
(Supplementary material: refer to PMC https://www.ncbi.nlm.nih.gov/pmc/journals/2350/)

the nerve network structure in the mucosa of the rat small intestine, and we comprehensively identified the types of cells that are in contact with nerve fibers [45]. Thus, while the nature and structure of the mucosal nerve network in the small intestine have been clarified in detail, much remains unknown about the mucosal nerve network in the large intestine.

Our previous study using SBF-SEM identified fibroblast-like cells (FBLCs) and macrophages as the cells being frequently in contact with the nerve fibers in the rat ileal mucosa [45]. Especially, contact between nerve fibers and FBLCs has also been observed by transmission electron microscopy [11, 24, 44]. FBLCs localized in the subepithelium release ATP in response to mechanical stimuli and transmit information to the intrinsic primary afferent neurons. Therefore, this physical contact between subepithelial FBLCs and nerve fibers is thought to be involved in mechanosensing in the intestinal villi [22, 23]. Thus, while the relationship between nerve fibers and FBLCs has been clarified in the small intestine, it is not clear whether they establish a universal relationship throughout the whole intestine including the large intestine. Furthermore, we recently showed that there are regional differences in the morphological characteristics, quantity and localization of subepithelial FBLCs and lamina propria FBLCs in the rat large intestine [55]. Therefore, it is possible that there are regional differences in the relationship between various kinds of cells in the mucosa, including FBLCs, and the mucosal nerve network throughout the large intestine. In this study, we performed immunohistochemistry against pan-neuronal marker, protein gene product 9.5 (PGP9.5), and various neurochemical markers (VIP, CR, VAChT, NPY, CGRP and SP) whose expressions have been frequently reported in the mucosal nerve network of the intestine [17, 18, 30, 36, 42], and SBF-SEM analysis to investigate the expression of various neuronal neurochemical markers, the structure of the nerve network, and the relationships between nerve fibers and cells in the mucosa in each region of the large intestine to clarify regional differences in the mucosal nerve network in the large intestine.

MATERIALS AND METHODS

Animals

Eight 7-week-old male Wistar rats (Japan SLC, Hamamatsu, Japan) were maintained under specific pathogen-free conditions in individual ventilated cages (Sealsafe Plus; Tecniplast, Bugugiate, Italy). They were permitted free access to water and food (Lab RA-2; Nosan Corp., Yokohama, Japan). The animal facility was maintained under a 12-hr/12-hr light/dark cycle at 23 ± 2°C and 50 ± 10% humidity. This animal study was approved by the Institutional Animal Care and Use Committee (permission no. 30-05-01) and carried out according to the Kobe University Animal Experimentation Regulations.

Tissue preparation for light microscopy

After euthanasia by overdose inhalation of isoflurane (Wako Junyaku, Osaka, Japan), tissue blocks were removed from the cecum, ascending colon and descending colon of 5 rats. Then, each block was immersion-fixed in 4.0% paraformaldehyde fixative in 0.1 M phosphate buffer for 6 hr at 4°C and snap-frozen in liquid nitrogen as described previously [39]. Sections were cut at a thickness of 4 µm using a Coldtome Leica CM1950 (Leica Biosystems, Nussloch, Germany), placed on slide glasses precoated with 0.2% 3-aminopropyltriethoxysilane (Shin-Etsu Chemical Co., Tokyo, Japan), and stored at −30°C until use.

Immunohistochemistry

For this investigation, enzyme immunohistochemical analysis was performed using a pan-neuronal marker and several neurochemical markers. Antigens were detected using the modified indirect method of enzyme immunohistochemistry with the antibodies. Briefly, the tissue sections were rinsed three times in 0.05% Tween-added 0.01 M phosphate-buffered saline (TPBS) after each preparation step to remove any reagent residues. All sections were then immersed in absolute methanol and 1.2% H_2O_2 for 30 min, respectively. Following blocking with Blocking One Histo (Nacalai Tesque Inc., Kyoto, Japan) for 1 hr at room temperature (r.t.), the sections were reacted with anti-PGP9.5 mouse IgG (diluted at 1:12,800, ab8189; Abcam, Cambridge, UK), anti-VIP mouse IgG (diluted at 1:3,200, ab30680; Abcam), anti-CR mouse IgG (diluted at 1:6,400, sc-365956; Santa Cruz biotechnology, Dallas, TX, USA), anti-VAChT rabbit IgG (diluted at 1:2,000, 139103; Synaptic Systems, Goettingen, Germany), anti-NPY mouse IgG (diluted at 1:6,400, GTX60971; GeneTex, Irvine, CA, USA), anti-CGRP goat IgG (diluted at 1:3,200, ab36001; Abcam) or anti-SP mouse IgG (diluted at 1:4,000, ab14184; Abcam), for 18 hr at 6°C. Next, the sections were incubated with HRP-conjugated anti-mouse IgG donkey IgG (diluted at 1:200, 715-035-151; Jackson ImmunoResearch Inc., West Grove, PA, USA), HRP-conjugated anti-rabbit IgG donkey IgG (diluted at 1:400, 715-035-152; Jackson ImmunoResearch Inc.) or HRP-conjugated anti-goat IgG donkey IgG (diluted at 1:200, 705–035-147; Jackson ImmunoResearch Inc.) for 1 hr at r.t. Sections were rinsed three times in TPBS and three times in Tris buffer (pH 7.6), and then stained in 0.02% 3,3′-diaminobenzidine (Dojindo Lab., Mashiki-machi, Japan) in Tris buffer with 0.17 µL/mL hydrogen peroxide solution. Control sections were incubated with TPBS or non-immunized mouse (sc-2025; Santa Cruz Biotechnology), rabbit (20009-1-200; Alpha Diagnostic International, San Antonio, TX, USA) or goat (500-G00; Pepro Tech EC, London, UK) IgG instead of the primary antibody, and these results were used to discriminate the specific reactions for each immunohistochemical analysis.

Acquisition of data stacks with SBF-SEM and 3D reconstruction of histological components

For this investigation, we reused the data stacks obtained from the portion around the intestinal crypt in our previous study [55] and additionally obtained the data from the luminal side of the cecum and descending colon using Sigma VP or Merlin (Carl Zeiss, Oberkochen, Germany) with a Gatan 3View 2XP system (Gatan, Abingdon, UK) (Supplementary Fig. 1). The tissue preparation procedures were described earlier [55]. The observation conditions in each tissue block were as follows: acceleration voltage, 1.2–1.5 kV; probe current, 130–164 pA; size in pixels, 8,192 × 8,192; X-Y resolution, 6 nm×6 nm; slice pitch, 100 nm; slice number, 392 or

more. Each data stack was aligned using Fiji. Alignment analyses for a portion of the data stacks were conducted after binning to a resolution of 12 nm.

Nerve fibers and nerve bundles including enteric glial cells, and the contact area with any of the types of cells in the mucosa, were three-dimensionally reconstructed from these aligned data stacks with the use of the program IMOD (https://bio3d.colorado.edu/imod/).

Measurement of the frequency of immunopositive structures

Images for the histological measurement were taken from the immunohistochemically stained tissue sections so that the entire lamina propria from the base of the intestinal crypt to the basal surface of intestinal superficial epithelial cells could be seen in the field of view. Image data were obtained with 6 to 10 fields of view per rat for each neurochemical marker. Only immunopositive areas were extracted using color deconvolution of Image J. The threshold function of Image J was set to eliminate the faint background positivity in the lamina propria in the negative control tissue sections when staining with mouse, rabbit or goat normal IgG. The immunopositive areas of various neurochemical markers were calculated using this threshold. Immunopositive areas were calculated in 1) the entire lamina propria and 2) the muscular and luminal quarter part of the lamina propria divided into four segments (Supplementary Fig. 2). Then, each frequency was calculated by dividing the area of each immunopositive structure by the area of the correspondent lamina propria (Supplementary Fig. 2).

Tentative classification of cells in contact with nerve fibers for the analysis of neural connectivity

Neural connectivity in the mucosa of the cecum and descending colon was analyzed according to the method used for the ileal mucosa in our previous study, with some modifications [45]. Briefly, FBLCs [38, 55], smooth muscle cells [55], macrophages (reported as macrophage like cells in the previous study [37]), plasma cells [37], and eosinophils [1] were defined based on our previous findings. Lymphocytes (reported as lymphocyte-like cells) and pericytes were defined using a definition similar to that in our previous study [45]. The type of some cells could not be identified; we thus refer to these cells as "undetermined" herein. In addition, we excluded enteric glial cells from the analysis objects, because the physical contacts between the enteric glial cells and nerve fibers were too numerous to count.

Quantitative histological analysis of SBF-SEM data

To compare the complexity of the network structure of nerve bundles, we measured the number of branches of the nerve bundle from one end or branching point to the next end or branching point as a single unit (Supplementary Fig. 3). After calculating the total area of the lamina propria included in each data stack by using a microscopy imaging browser [3], the number of nerve bundle units per unit area of lamina propria were calculated (Supplementary Fig. 3 and Supplementary Table 1). We then counted the number of cells that were in contact with one or more nerve fibers. In addition, we reconstructed the three-dimensional contact structures of nerve fibers and counted the number of contact structures swollen to a maximum diameter of 1 μm or more and those not swollen. Finally, we traced the outline of all the above contact sites by nerve fibers and measured the area of these contact sites using a microscopy imageing browser. These results are presented as numerical data.

Statical analysis

The normality of distribution was first assessed by the Kolmogorov–Smirnov test. For non-parametric variables in the comparison between two groups, a Mann–Whitney *U* test was performed. For non-parametric variables in multiple comparisons, a Kruskal–Wallis test was performed with the Steel–Dwass test as a *post-hoc* test. *P* values less than 0.05 were considered statistically significant. The statistical methods used in each analysis are described in the figure legends.

RESULTS

Immunohistochemistry for neurochemical markers

The immunopositive reactions against VIP, NPY, VAChT, CGRP, and SP were observed mainly as minute-granular structures, whereas those against PGP9.5, a pan-neuronal marker, and CR were observed as either fibrous or granular structures in the lamina propria of any of the regions studied (i.e., the rat cecum, ascending colon or descending colon; Fig. 1). These immunopositive structures for each marker were found in the whole lamina propria in all regions of the large intestine. Immunopositive reactions for SP and CGRP were less frequent than those for other neurochemical markers.

We next quantified differences in the frequency of the immunopositive structures among the cecum, ascending and descending colon. The frequency of PGP9.5$^+$ structures in the lamina propria was highest in the ascending colon and not significantly different between the cecum and descending colon. In addition, the frequencies of VIP$^+$, CR$^+$, and VAChT$^+$ structures in the lamina propria were also highest in the ascending colon, although in the case of the VAChT$^+$ structures the difference was not significantly different. Comparing the cecum and descending colon, the frequency of VIP$^+$ structures was significantly higher in the cecum, while the frequency of VAChT$^+$ structures was higher in the descending colon, although not significantly. The frequencies of NPY$^+$, CGRP$^+$, and SP$^+$ structures did not differ significantly among regions (Fig. 2a). Comparing the frequency of structures immunopositive for the different neurochemical markers between the muscular and luminal sides of each region, the frequencies of PGP9.5$^+$ and VIP$^+$ structures were higher on the muscular side, especially in the cecum. The frequency of SP$^+$ structures was significantly higher on the muscular side, especially in the ascending colon, whereas that of CR$^+$ structures was significantly higher on the luminal side, especially in the descending colon (Fig. 2b). No notable differences were detected between the muscular side and the luminal side for the other neurochemical markers.

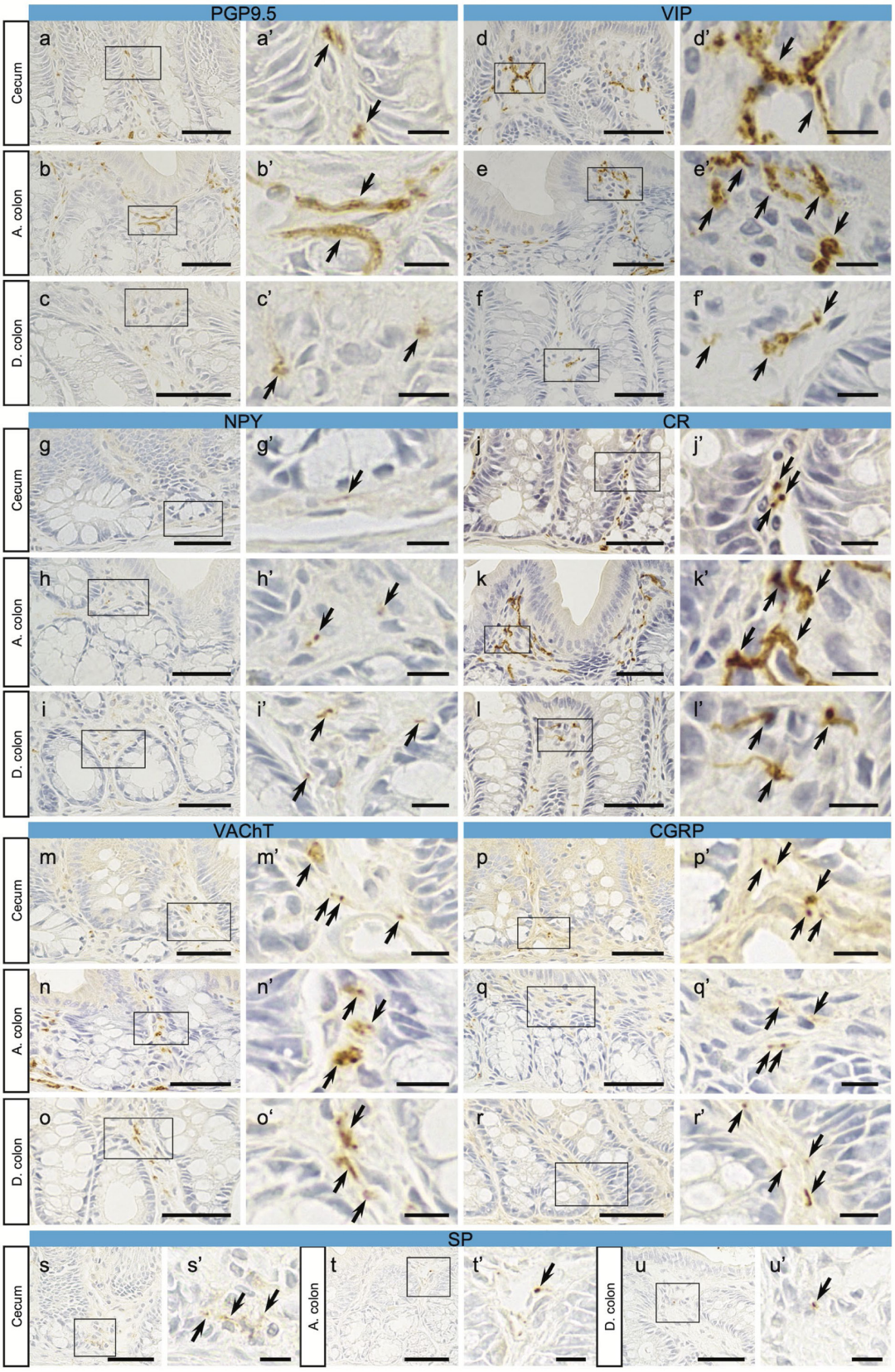

Fig. 1. Images of immunohistochemistry for various neurochemical markers in the rat cecum (a, d, g, j, m, p, s), ascending colon (A. colon) (b, e, h, k, n, q, t) and descending colon (D. colon) (c, f, i, l, o, r, u). Granular or fibrous immunopositive structures for protein gene product 9.5 (PGP9.5) (**a–c**), vasoactive intestinal peptide (VIP) (**d–f**), neuropeptide Y (NPY) (**g–i**), calretinin (CR) (**j–l**), vesicular acetylcholine transporter (VAChT) (**m–o**), calcitonin gene-related peptide (CGRP) (**p–r**), and substance P (SP) (**s–u**) are observed in the lamina propria of each region in the large intestine. Panels 1a'–u' are high-magnification images of the square area in panels 1a-u, respectively. (a–u) Bar=50 µm. (a'–u') Bar=10 µm.

3D analysis of the mucosal nerve network in the rat large intestine

The above analysis suggested that the immunohistochemical characteristics of the mucosal nerve network of the cecum and that of the descending colon were relatively similar, except with respect to the frequency of VIP$^+$ structures. Therefore, we next investigated potential differences in the structure of the mucosal nerve network between the cecum and descending colon by means of three-dimensional analysis using SBF-SEM. As a result, we found that the nerve bundles, identified and reconstructed as in our previous study [45], formed networks by branching/anastomosing in the lamina propria in the rat cecum and descending colon (Fig.

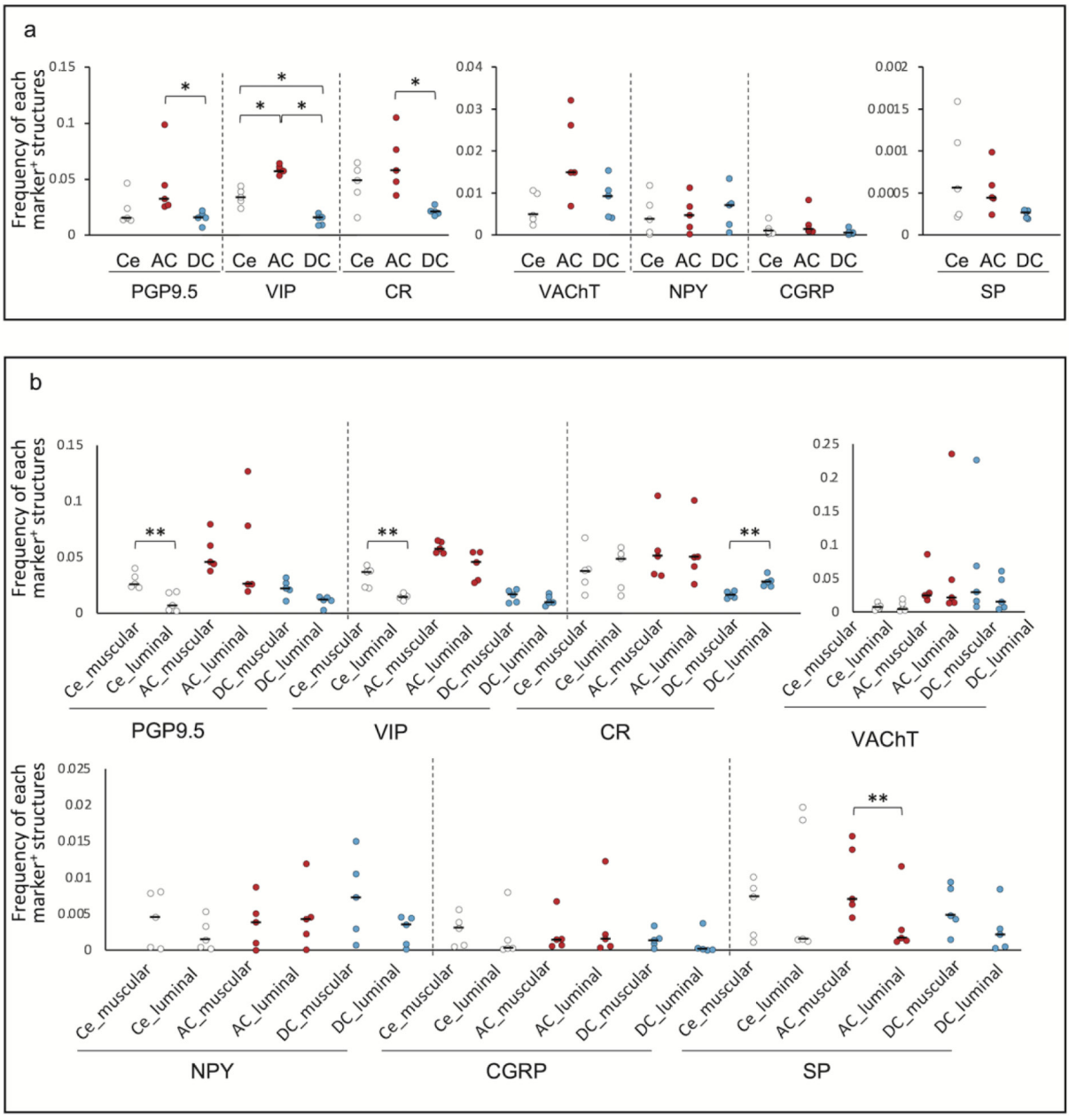

Fig. 2. **a:** The frequency of structures immunopositive for each neurochemical marker in the whole lamina propria of the cecum, ascending colon and descending colon. **b:** The frequency of structures immunopositive for each neurochemical marker on the muscular side (muscular) and the luminal side (luminal) of the cecum, ascending colon, and descending colon. AC, ascending colon; Ce, cecum; CGRP, calcitonin gene-related peptide; CR, calretinin; DC, descending colon; NPY, neuropeptide Y; PGP9.5, protein gene product 9.5; SP, substance P; VAChT, vesicular acetylcholine transporter; VIP, vasoactive intestinal peptide. Each median value is represented by a horizontal bar. Double asterisks, $P<0.01$. Asterisk, $P<0.05$ (**a:** Kruskal–Wallis test with Steel–Dwass test; **b**: Mann–Whitney U test). n=5.

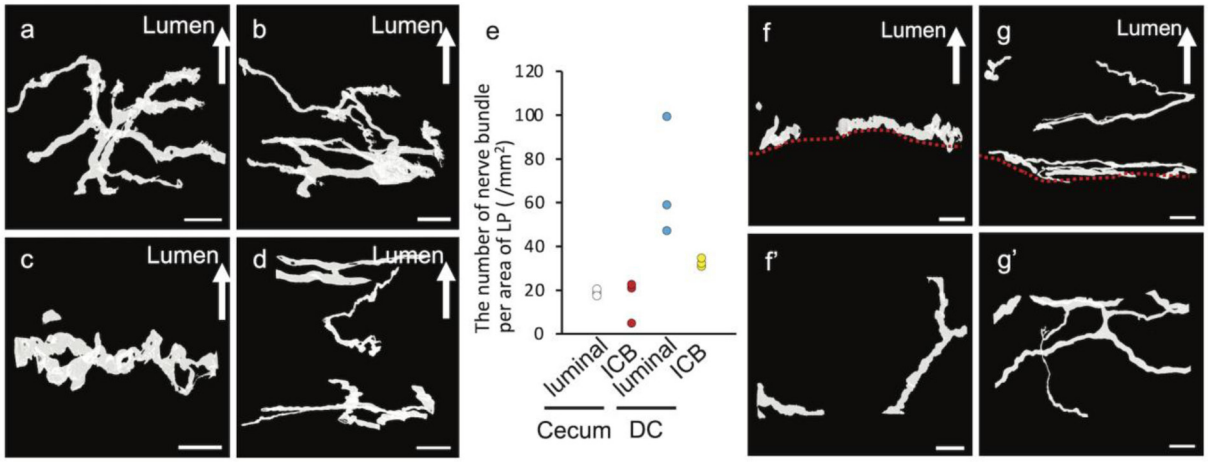

Fig. 3. **a-d:** 3D images of the running pattern of nerve bundles, including both nerve fibers and enteric glial cells. The upper parts of each image are the luminal side of the intestine (white arrows). Nerve bundles (light gray) run with branching/anastomosing in the lamina propria on the luminal side (a, b) and around the intestinal crypt base (c, d) of the cecum (a, c) and descending colon (b, d). **e:** Complexity of the nerve network in the lamina propria (LP) around the intestinal crypt base (ICB) and on the luminal side (luminal) of the cecum and descending colon (DC). **f, g:** Nerve bundles (light gray) run along the muscularis mucosae (red dashed line) of the cecum (f) and descending colon (g). Upper parts of images are the luminal side of the intestine (white arrows). Panels 3f' and g' are three-dimensional images of only the nerve bundles running along the muscularis mucosae of panels 3f and g, respectively, rotated 90 degrees and observed from the luminal side. Bar=10 µm.

3a–d). To compare the complexity of the network structure of nerve bundles, we counted the number of nerve bundles within each unit area of the lamina propria; nerve bundles between one end or branching point and the next end or branching point were counted as a single unit (Supplementary Fig. 3). The results showed that the nerve network in the lamina propria of the descending colon was more complex than that in the cecum (Fig. 3e). In the cecum, there was no apparent difference between the lamina propria around the intestinal crypt base and that on the luminal side (Fig. 3e). On the other hand, in the descending colon, there were more branchings/anastomoses in the lamina propria on the luminal side than around the intestinal crypt base (Fig. 3e). Nerve bundles running along muscularis mucosae were observed around the intestinal crypt base in both the cecum and the descending colon (Fig. 3f–g). This nerve network along the muscularis mucosae was more developed in the descending colon than in the cecum (Fig. 3f–g).

Analysis of the connectivity of nerve fibers in the mucosa of the rat large intestine

We next analyze the physical contact between nerve fibers and each kind of cells in the mucosa. We qualified visible gapless relationships between the surface membrane of the nerve fiber and each cell in the mucosa at a resolution of 12 nm or less as "contact". In data stacks in this study, both the cecum and descending colon, nerve fibers were in physical contact with the various cells in the lamina propria, but not with any epithelial cells as shown below. Considering that the connectivity of the nerve fibers is important for interpreting the function in the mucosal nerve network as discussed in the previous study [45], we next quantitatively analyzed both the number of these cells which were in contact with nerve fibers (hereinafter "contact cells") and the area of contact between the "contact cells" and nerve fibers.

Careful tracing of the nerve bundles and individual nerve fibers in all data stacks revealed that subepithelial FBLCs, lamina propria FBLCs, and macrophages were major contact cells, while plasma cells, lymphocytes, eosinophils, pericytes and smooth muscle cells were minor contact cells (Fig. 4c–h, Table 1, Supplementary Fig. 4, Supplementary Table 2). In both the cecum and descending colon, contact cells were abundantly detected in the lamina propria on the luminal side (cecum: 43.13 ± 5.91; descending colon: 25.2 ± 5.05), while contact cells were scarcely found around the intestinal crypt base (cecum: 2.60 ± 1.40; descending colon: 4.26 ± 1.52) (Table 1). Nerve fibers were more frequently in contact with subepithelial FBLCs on the luminal side of the cecum than that of the descending colon, while these contacts were scarce around the intestinal crypt base in both regions. Nerve fibers of the cecum were in contact with lamina propria FBLCs only on the luminal side, while lamina propria FBLCs were the most common contact cells both on the luminal side and around the intestinal crypt base in the descending colon. Contact between nerve fibers and macrophages on the luminal side was more than twice as frequent in the cecum than in the descending colon in any rat (Supplementary Table 2), while such contact around the intestinal crypt base was found only in the descending colon. Contact with plasma cells and eosinophils was observed only in the cecum, although there was no difference in the quantity of contact with lymphocytes between the cecum and descending colon (Table 1).

Next, we reconstructed the three-dimensional contact structures of nerve fibers and found out that nerve fibers were sometimes swelled like varicosities at contact sites (Fig. 4b, Supplementary Fig. 5) as same as the previous study [45]. We therefore quantified the number of swelled contact structures (maximum diameter ≥1 µm) and non-swelled contact structures. These swelled contact structures of nerve fibers normally contained synaptic vesicle-like structures (Fig. 4a). In both the cecum and descending colon, swelled

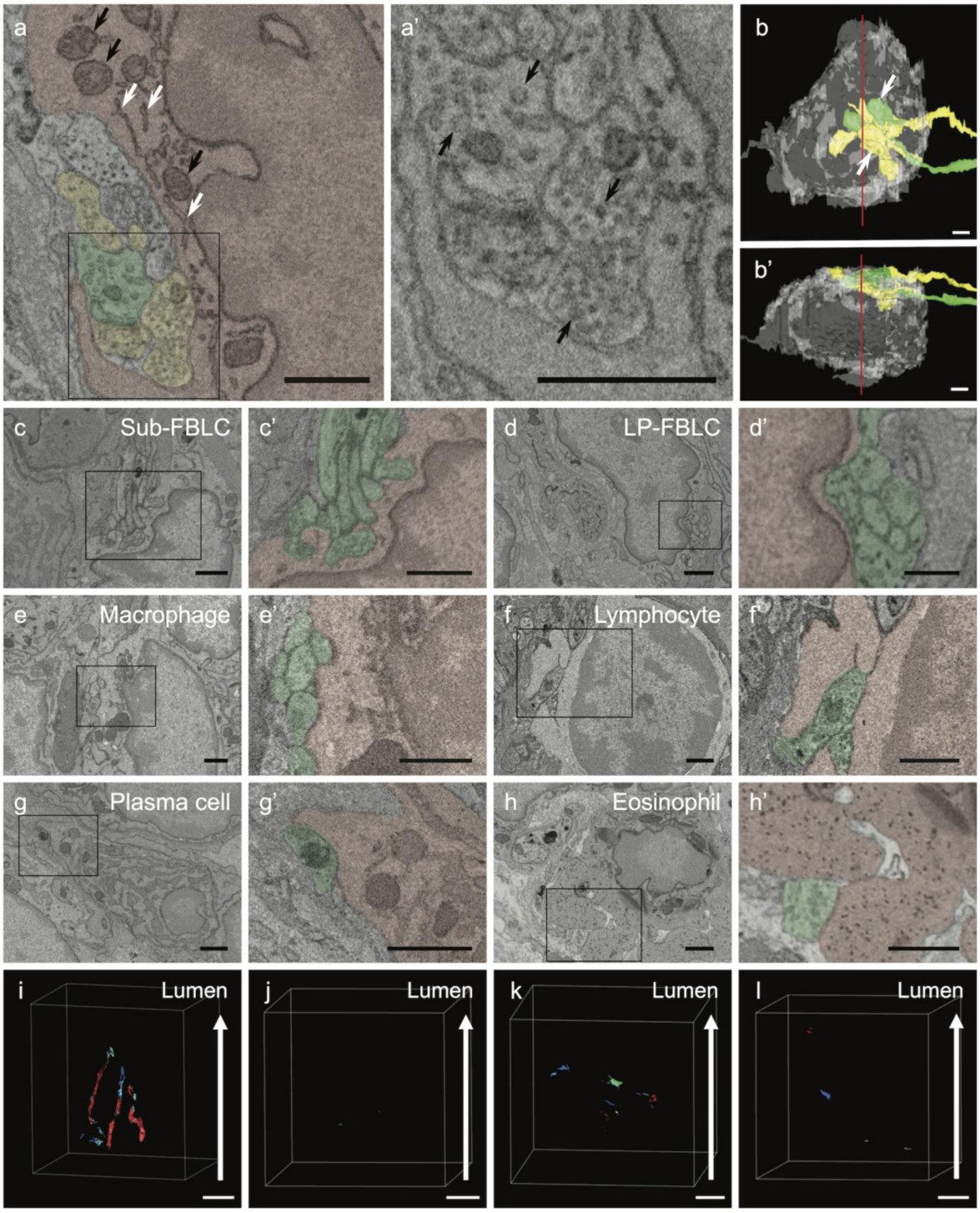

Fig. 4. Ultrastructural observation of contacts between nerve fibers and contact cells. **a:** Nerve fibers are in contact with a lymphocyte (red) in the lamina propria. Two of them are colored by green and yellow, respectively. Mitochondria (black arrows) and endoplasmic reticulum (white arrows) are seen in a lymphocyte. **a':** High-magnification image of the square area in panel 4a. Synaptic vesicle-like structures (arrows) are observed in nerve fibers. **b–b':** Three-dimensional images of the contact site of the nerve fiber in panel 4a. The nerve fibers (green and yellow) are in contact with a lymphocyte (grey) and swelled like varicosity (arrows) at contact site. The cross-sectional image at the red line in panel 4b is panel 4a. The color of each nerve fiber in panel 4b corresponds to the color in panel 4a. Panel 4b' is the image rotated 90 degrees from panel 4b. Three-dimensional images of individual nerve fiber are shown in Supplementary Fig. 5. **c–h:** Nerve fibers (green) in contact with a subepithelial fibroblast-like cell (Sub-FBLC) (c, red), lamina propria FBLC (LP-FBLC) (d, red), macrophage (e, red), lymphocyte (f, red), plasma cell (g, red), and eosinophil (h, red). Panels 4a' and c'–h' are high-magnification images of the squares in panels 4a and c-h, respectively. **i–l:** Three-dimensional images of the contact sites between nerve fibers and cells in the mucosa of the cecum (i, j) and descending colon (k, l). More extensive contacts are seen on the luminal side (i, k) compared to the portion around the intestinal crypt base (j, l) in both the cecum (i, j) and descending colon (k, l). The contact sites of nerve fibers are particularly wide on the luminal side of the cecum (i). Red, blue and green materials indicate the contact sites between nerve fibers and macrophages, FBLCs, and other cells, respectively. **a–h:** Bar=1 µm. **i-l:** Bar=10 µm.

Table 1. The number of cells which were in contact with nerve fibers in the lamina propria of the cecum and the descending colon

Class	Cell type	Cecum		Descending colon	
		L	ICB	L	ICB
FBLC	Sub-FBLC	12.05 ± 2.33	0.50 ± 0.50	6.96 ± 4.97	0
	LP-FBLC	7.57 ± 1.51	0	8.90 ± 1.49	1.91 ± 0.99
Immuno-competent cell	Macrophage	18.31 ± 4.06	0	5.69 ± 1.72	1.18 ± 0.03
	Plasma cell	1.26 ± 1.26	0.53 ± 0.53	0	0
	Lymphocyte	1.55 ± 0.99	0	2.31 ± 1.79	0
	Eosinophil	0.42 ± 0.42	1.06 ± 1.06	0	0
Others	Pericyte	0	0.50 ± 0.50	0	0
	Smooth muscle cell	0.42 ± 0.42	0	0.37 ± 0.37	0.40 ± 0.40
Undetermined		1.55 ± 0.99	0	0.97 ± 0.97	0.77 ± 0.39
Total		43.13 ± 5.91	2.60 ± 1.40	25.2 ± 5.05	4.26 ± 1.52

The number of cells whose nuclei were completely included in the data stacks was counted. Numbers represent the number of cells which were in contact with nerve fibers per area of lamina propria (mm^2). Data are presented as mean ± SE. n=3. L, portion on the luminal side; ICB, portion around the intestinal crypt base; FBLC, fibroblast-like cell; Sub-FBLC, subepithelial FBLC; LP-FBLC, lamina propria FBLC.

Table 2. The number of contact structures of nerve fibers which were in contact with mucosal cells in the cecum or the descending colon

Class	Cell type	Cecum		Descending colon	
		L	ICB	L	ICB
FBLC	Sub-FBLC	43 (9)	2 (2)	25 (6)	0
	LP-FBLC	45 (19)	0	58 (23)	19 (12)
Immuno-competent cell	Macrophage	163 (58)	0	60 (32)	8 (2)
	Plasma cell	2 (1)	1 (0)	0	0
	Lymphocyte	4 (2)	0	17 (5)	0
	Eosinophil	3 (3)	2 (2)	0	0
Others	Pericyte	0	1 (1)	0	0
	Smooth muscle cell	2 (1)	0	4 (2)	1 (0)
Undetermined		13 (7)	0	3 (1)	3 (1)
Total		275 (100)	6 (5)	167 (69)	31 (15)

Numbers in parentheses are the numbers of swelling structures. L, portion on the luminal side; ICB, portion around the intestinal crypt base; FBLC, fibroblast-like cell; Sub-FBLC, subepithelial FBLC; LP-FBLC, lamina propria FBLC.

contact structures were more frequently found in the luminal side than around the intestinal crypt base. Swelled contact structures were frequently found in the contact structures against lamina propria FBLCs and macrophages (Table 2). Interestingly, the number of swelled contact structures against macrophages was more than half of the number of total swelled contact structures in the cecum. On the other hand, most of contact structures against subepithelial FBLCs, which were the main contact cells along with lamina propria FBLCs and macrophages in any regions (Table1), were not swelled (Table 2).

Finally, we measured the area of nerve fibers in contact with each contact cell as the "contact area", and determined the contact area per unit area of the lamina propria (Table 3). In both the cecum and the descending colon, total contact area on the luminal side was larger than that around the intestinal crypt base. In particular, the contact area in the lamina propria of the luminal side of the cecum was by far the largest among the portions (Fig. 4i–l). As expected, the contact area with the major contact cells (subepithelial FBLCs, lamina propria FBLCs, and macrophages) was larger than the contact area with most of other types of cells (Table 3). The contact area with macrophages was larger in the lamina propria of the luminal side in the cecum than that of other cell types in any portion (Table 3). In addition, the contact area with both subepithelial FBLCs and lamina propria FBLCs was larger in the lamina propria of the luminal side of the cecum than that of the descending colon (Table 3).

DISCUSSION

The enteric mucosal functions, such as intestinal fluid secretion [16] and antibacterial agent secretion [51] are considered to be regulated by enteric mucosal nerve network. Therefore, understanding how the mucosal nerve network is formed in each region of the intestine is important to understand the region-specific functions of the mucosal nerve network. In this study, we investigated this matter using a combination of SBF-SEM analysis and histological analysis by immunohistochemistry against various neurochemical markers. Our results suggested that the mucosal nerve network in the large intestine possesses both regional universalities and

Table 3. The total area of contact sites between nerve fibers and each type of cells per the area of total lamina propria in the cecum and the descending colon

Class	Cell type	Cecum		Descending colon	
		L	ICB	L	ICB
FBLC	Sub-FBLC	4,818,317	75,551	1,941,314	0
	LP-FBLC	5,641,513	0	3,235,673	6,536
Immuno-competent cell	Macrophage	31,442,938	0	4,575,597	480
	Plasma cell	221,739	107,371	0	0
	Lymphocyte	195,621	0	2,415,050	0
	Eosinophil	305,698	71,146	0	0
Others	Pericyte	0	35,409	0	0
	Smooth muscle cell	106,798	0	165,968	24
Undetermined		2,239,602	0	172,145	403
Total		42,732,628	289,479	12,333,604	7,040

Numbers represent the total area of the contact sites between nerve fibers and each type of cells (μm^2) per area of total lamina propria (μm^2), and are multiplied by 10^{12}. L, portion on the luminal side; ICB, portion around the intestinal crypt base; FBLC, fibroblast-like cell; Sub-FBLC, subepithelial FBLC; LP-FBLC, lamina propria FBLC.

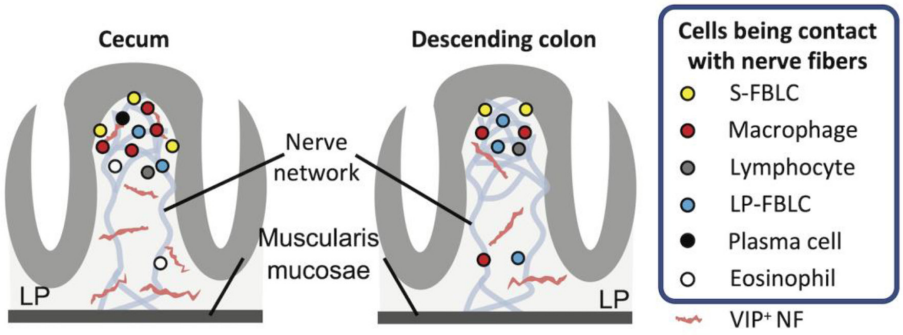

Fig. 5. Schematic diagram of the histological characteristics of the mucosal nerve network in the cecum and descending colon. FBLC, fibroblast-like cell; LP, lamina propria; NF, nerve fiber; S, subepithelial; VIP, vasoactive intestinal peptide.

specificities in terms of its structure, expression pattern of neurochemical markers, and patterns of physical contact with mucosal cells (Fig. 5). The details are discussed below.

Over the last decade, volume electron microscopy techniques have been used to analyze the neural connectome in general [46], as well as the specific neural connectivity in the neocortex [29], visual cortex [35], thalamus [43] and retina [25]. Our previous studies using the volume electron microscopy technique known as SBF-SEM comprehensively elucidated the types of cells which were in contact with nerve fibers in the rat ileal mucosa [45]. In this study, we applied this technique to the analysis of nerve networks in the mucosa of the large intestine. Our results showed that the nerve network structure in the mucosa of the descending colon was more complex on the luminal side than around the intestinal crypt base. In addition, nerve fibers were in contact with various types of cells in the cecum and descending colon in this study as same as the previous study using the rat ileum [45]. These findings support the study by transmission electron microscopy which have clarified that nerve fibers are in contact with FBLCs [11, 24, 44] and mononuclear phagocytes [8] in the intestinal mucosa. Neurotransmission by the peripheral autonomic nervous system is thought to act in diffusion manner from swelled structures of the nerve fibers, called varicosity, not by synapse [28]. It has been considered that nerve network in the intestinal tract regulates the function of target cells in the volume transmission manner [50]. However, given that swelled contact structures of nerve fibers, reminiscent of varicosity, were frequently in contact with lamina propria FBLCs and macrophages in the large intestine in the present study, it is hypothesized that nervous control in the intestinal mucosa is possibly mediated not only by volume transmission but also by physical contact-dependent manner. If so, physical contact between nerve fibers and contact cells may enable cell-by-cell nervous control in the intestinal mucosa, where various types of cells exist in abundance. Unfortunately, SBF-SEM analysis in the present study could not obtain finer ultrastructure at the contact sites, because SBF-SEM cannot repeatedly image the same site. Further investigation will be needed to examine the above hypothesis by repeatedly-analyzable volume electron microscopy technique such as automatic tape-collecting ultra-microtome SEM.

Moreover, contact cells that were in contact with nerve fibers were more abundant on the luminal side, and the major contact cells were the subepithelial and lamina propria FBLCs and macrophages. Studies using transmission electron microscopy have reported similar results in the small intestine [for FBLCs: (11, 24, 44) for mononuclear phagocytes: (8)]. Moreover, our above two findings common in both the cecum and the descending colon were also similar to the findings in the rat ileum in our previous study [45]. Collectively, these results suggest that the mucosal nerve network develops universally as a highly complex network on the luminal

side and functions to regulate the activities of FBLCs and macrophages. Subepithelial FBLCs in particular have been shown to function as mechanosensor in the intestinal villi in the small intestine [22, 23]. Considering that nerve fibers were in abundant contact with FBLCs on the luminal side of the cecum and descending colon in the present study, the dense interaction network between FBLCs and the mucosal nerves might function as a mechanosensing system throughout the entire intestinal mucosa, especially on the luminal side, which receives abundant physical stimulation.

The mucosal nerve network has been reported to regulate various activities of epithelial cells, such as their proliferation [6, 27] and their secretion of intestinal fluid [13, 16, 20]. In fact, VIP^+ nerve fibers, which are considered to be extended from the secretomotor neurons [20], run immediately beneath epithelial cells [2]. In the present study, however, nerve fibers were not in contact with any epithelial cells, at least in the cecum and descending colon. Instead, nerve fibers were in contact with lamina propria FBLCs around the intestinal crypt base of the descending colon in our data stacks. These lamina propria FBLCs were considered to correspond to $CD34^+$ FBLCs in the rat large intestine, and $CD34^+$ FBLCs around the crypt were more highly abundant in the descending colon than in the cecum [55]. $CD34^+gp38^+$ stromal cells around the intestinal crypt have been reported to express Wnt, R-spondin1 and gremlin [54], which are regulators of epithelial stem cell maintenance [12, 32, 47, 54]. Based on the above findings, the abundant contact between nerve fibers and lamina propria FBLCs in the descending colon observed herein suggests that the nerve network might regulate the maintenance of epithelial stem cells through lamina propria FBLCs around the intestinal crypt of the descending colon.

Nerve fibers running in the intestinal mucosa mainly originate from either the intrinsic non-cholinergic or cholinergic secretomotor neurons [9, 15, 16, 19, 31], intrinsic primary afferent neurons (IPANs) [7, 15, 21, 36], extrinsic sympathetic neurons [10, 14, 15] or extrinsic primary afferent neurons [4, 5, 15, 41, 57]. Immunohistochemical analysis in the present study revealed that there were not regional differences in the immunopositivity against CGRP, SP, and NPY. CGRP and SP are known to be expressed in both intrinsic and extrinsic primary afferent neurons [7, 15, 21, 36, 48, 56], while NPY is known to be expressed in sympathetic neuron [40, 53, 56]. From these findings, sensory neuron and sympathetic neuron-derived nerve fibers are suggested to be developed to the same level in the mucosa in each region of the rat large intestine. On the other hand, the expression of VIP, which is known to be expressed in non-cholinergic secretomotor neurons [19, 42], was higher in order of the ascending colon, cecum and descending colon, while that of VAChT, which is the marker of the cholinergic neuron [49, 58] such as cholinergic secretomotor neurons [15, 26, 31], did not significantly differ between regions. This finding suggests that the regional difference of mucosal nerve network in the large intestine is generated by VIP^+ non-cholinergic secretomotor neurons. Considering that VIP^+ nerve fibers were more abundant in the cecum than the descending colon and that the majority of swelled contact structures in the cecum were in contact with the macrophages, the relationship between macrophages and VIP^+ nerves in the cecum is a fascinating topic to be analyzed in the future.

SBF-SEM analysis in the present study revealed the relationship between the mucosal nerve network and immune cells in the rat large intestine. Nerve fibers were more frequently in contact with macrophages in the cecum than in the descending colon as discussed above. Nerve fibers being in contact with lymphocytes was observed in both the cecum and the descending colon, whereas those being in contact with plasma cells and eosinophils were detected only in the cecum. These results suggest that there is a regional difference in the type of immune cells regulated by the mucosal nerve network in the rat large intestine. There are many lymphoid tissues including isolated and aggregated lymphoid follicles in the animal intestine. Nerve network in Peyer's parch is developed especially in the interfollicular area which is T cell area [33, 34]. Unfortunately, the data stacks used in this study did not contain any lymphoid tissue, but SBF-SEM analysis must be useful to uncover the relationship between nerve network and lymphocytes or the other immune cells in the lymphoid follicles.

In conclusion, this study revealed that the mucosal nerve network in the large intestine possessed both universal and region-specific characteristics in terms of the nerve network structure in the mucosa, the immunohistochemical characteristics of the nerve network, and the cells which were in contact with the nerve fibers, and that the mucosal nerve network was in abundant contact with immune cells in the cecum. These regional differences in the nerve network should lead to region-specific functions of the mucosal nerve network of the large intestine, which is an attractive hypothesis to examine in the future.

CONFLICT OF INTEREST. The authors declare that they have no conflict of interest associated with this manuscript.

ACKNOWLEDGMENTS. This work was supported by JSPS KAKENHI Grants (nos. JP16K18813, JP16H06280, JP20K15902 and JP22J10350) and by the Cooperative Study Program of the National Institute for Physiological Sciences.

REFERENCES

1. Arai M, Mantani Y, Nakanishi S, Haruta T, Nishida M, Yuasa H, Yokoyama T, Hoshi N, Kitagawa H. 2020. Morphological and phenotypical diversity of eosinophils in the rat ileum. *Cell Tissue Res* **381**: 439–450. [Medline] [CrossRef]
2. Balemba OB, Grøndahl ML, Mbassa GK, Semuguruka WD, Hay-Smith A, Skadhauge E, Dantzer V. 1998. The organisation of the enteric nervous system in the submucous and mucous layers of the small intestine of the pig studied by VIP and neurofilament protein immunohistochemistry. *J Anat* **192**: 257–267. [Medline] [CrossRef]
3. Belevich I, Joensuu M, Kumar D, Vihinen H, Jokitalo E. 2016. Microscopy Image Browser: a platform for segmentation and analysis of multidimensional datasets. *PLoS Biol* **14**: e1002340. [Medline] [CrossRef]
4. Berthoud HR, Kressel M, Raybould HE, Neuhuber WL. 1995. Vagal sensors in the rat duodenal mucosa: distribution and structure as revealed by in vivo DiI-tracing. *Anat Embryol (Berl)* **191**: 203–212. [Medline] [CrossRef]
5. Berthoud HR, Patterson LM. 1996. Anatomical relationship between vagal afferent fibers and CCK-immunoreactive entero-endocrine cells in the rat small intestinal mucosa. *Acta Anat (Basel)* **156**: 123–131. [Medline] [CrossRef]

6. Bjerknes M, Cheng H. 2001. Modulation of specific intestinal epithelial progenitors by enteric neurons. *Proc Natl Acad Sci USA* **98**: 12497–12502. [Medline] [CrossRef]
7. Bornstein JC, Furness JB, Costa M. 1989. An electrophysiological comparison of substance P-immunoreactive neurons with other neurons in the guinea-pig submucous plexus. *J Auton Nerv Syst* **26**: 113–120. [Medline] [CrossRef]
8. Buckinx R, Alpaerts K, Pintelon I, Cools N, Van Nassauw L, Adriaensen D, Timmermans JP. 2017. In situ proximity of CX3CR1-positive mononuclear phagocytes and VIP-ergic nerve fibers suggests VIP-ergic immunomodulation in the mouse ileum. *Cell Tissue Res* **368**: 459–467. [Medline] [CrossRef]
9. Cooke HJ, Sidhu M, Wang YZ. 1997. Activation of 5-HT1P receptors on submucosal afferents subsequently triggers VIP neurons and chloride secretion in the guinea-pig colon. *J Auton Nerv Syst* **66**: 105–110. [Medline] [CrossRef]
10. Costa M, Furness JB. 1984. Somatostatin is present in a subpopulation of noradrenergic nerve fibres supplying the intestine. *Neuroscience* **13**: 911–919. [Medline] [CrossRef]
11. Desaki J, Fujiwara T, Komuro T. 1984. A cellular reticulum of fibroblast-like cells in the rat intestine: scanning and transmission electron microscopy. *Arch Histol Jpn* **47**: 179–186. [Medline] [CrossRef]
12. Farin HF, Van Es JH, Clevers H. 2012. Redundant sources of Wnt regulate intestinal stem cells and promote formation of Paneth cells. *Gastroenterology* **143**: 1518–1529.e7. [Medline] [CrossRef]
13. Field M. 2003. Intestinal ion transport and the pathophysiology of diarrhea. *J Clin Invest* **111**: 931–943. [Medline] [CrossRef]
14. Furness JB. 1970. The origin and distribution of adrenergic nerve fibres in the guinea-pig colon. *Histochemie* **21**: 295–306. [Medline] [CrossRef]
15. Furness JB. 2000. Types of neurons in the enteric nervous system. *J Auton Nerv Syst* **81**: 87–96. [Medline] [CrossRef]
16. Furness JB. 2012. The enteric nervous system and neurogastroenterology. *Nat Rev Gastroenterol Hepatol* **9**: 286–294. [Medline] [CrossRef]
17. Furness JB, Costa M, Emson PC, Håkanson R, Moghimzadeh E, Sundler F, Taylor IL, Chance RE. 1983. Distribution, pathways and reactions to drug treatment of nerves with neuropeptide Y- and pancreatic polypeptide-like immunoreactivity in the guinea-pig digestive tract. *Cell Tissue Res* **234**: 71–92. [Medline] [CrossRef]
18. Furness JB, Costa M, Gibbins IL, Llewellyn-Smith IJ, Oliver JR. 1985. Neurochemically similar myenteric and submucous neurons directly traced to the mucosa of the small intestine. *Cell Tissue Res* **241**: 155–163. [Medline] [CrossRef]
19. Furness JB, Costa M, Keast JR. 1984. Choline acetyltransferase- and peptide immunoreactivity of submucous neurons in the small intestine of the guinea-pig. *Cell Tissue Res* **237**: 329–336. [Medline] [CrossRef]
20. Furness JB, Jones C, Nurgali K, Clerc N. 2004. Intrinsic primary afferent neurons and nerve circuits within the intestine. *Prog Neurobiol* **72**: 143–164. [Medline] [CrossRef]
21. Furness JB, Trussell DC, Pompolo S, Bornstein JC, Smith TK. 1990. Calbindin neurons of the guinea-pig small intestine: quantitative analysis of their numbers and projections. *Cell Tissue Res* **260**: 261–272. [Medline] [CrossRef]
22. Furuya K, Sokabe M, Furuya S. 2005. Characteristics of subepithelial fibroblasts as a mechano-sensor in the intestine: cell-shape-dependent ATP release and P2Y1 signaling. *J Cell Sci* **118**: 3289–3304. [Medline] [CrossRef]
23. Furuya S, Furuya K. 2013. Roles of substance P and ATP in the subepithelial fibroblasts of rat intestinal villi. *Int Rev Cell Mol Biol* **304**: 133–189. [Medline] [CrossRef]
24. Güldner FH, Wolff JR, Keyserlingk DG. 1972. Fibroblasts as a part of the contractile system in duodenal villi of rat. *Z Zellforsch Mikrosk Anat* **135**: 349–360. [Medline] [CrossRef]
25. Helmstaedter M, Briggman KL, Turaga SC, Jain V, Seung HS, Denk W. 2013. Connectomic reconstruction of the inner plexiform layer in the mouse retina. *Nature* **500**: 168–174. [Medline] [CrossRef]
26. Hens J, Schrödl F, Brehmer A, Adriaensen D, Neuhuber W, Scheuermann DW, Schemann M, Timmermans JP. 2000. Mucosal projections of enteric neurons in the porcine small intestine. *J Comp Neurol* **421**: 429–436. [Medline] [CrossRef]
27. Hoffmann P, Mazurkiewicz J, Holtmann G, Gerken G, Eysselein VE, Goebell H. 2002. Capsaicin-sensitive nerve fibres induce epithelial cell proliferation, inflammatory cell immigration and transforming growth factor-alpha expression in the rat colonic mucosa in vivo. *Scand J Gastroenterol* **37**: 414–422. [Medline] [CrossRef]
28. Kandel ER, Schwartz JH, Jessel TM. 2000. Principles of Neural Science, 4th ed., McGraw-Hill, New York.
29. Kasthuri N, Hayworth KJ, Berger DR, Schalek RL, Conchello JA, Knowles-Barley S, Lee D, Vázquez-Reina A, Kaynig V, Jones TR, Roberts M, Morgan JL, Tapia JC, Seung HS, Roncal WG, Vogelstein JT, Burns R, Sussman DL, Priebe CE, Pfister H, Lichtman JW. 2015. Saturated reconstruction of a volume of neocortex resource saturated reconstruction of a volume of neocortex. *Cell* **162**: 648–661. [Medline] [CrossRef]
30. Keast JR, Furness JB, Costa M. 1984. Origins of peptide and norepinephrine nerves in the mucosa of the guinea pig small intestine. *Gastroenterology* **86**: 637–644. [Medline] [CrossRef]
31. Keast JR, Furness JB, Costa M. 1985. Investigations of nerve populations influencing ion transport that can be stimulated electrically, by serotonin and by a nicotinic agonist. *Naunyn Schmiedebergs Arch Pharmacol* **331**: 260–266. [Medline] [CrossRef]
32. Kosinski C, Li VS, Chan AS, Zhang J, Ho C, Tsui WY, Chan TL, Mifflin RC, Powell DW, Yuen ST, Leung SY, Chen X. 2007. Gene expression patterns of human colon tops and basal crypts and BMP antagonists as intestinal stem cell niche factors. *Proc Natl Acad Sci USA* **104**: 15418–15423. [Medline] [CrossRef]
33. Krammer HJ, Kühnel W. 1993. Topography of the enteric nervous system in Peyer's patches of the porcine small intestine. *Cell Tissue Res* **272**: 267–272. [Medline] [CrossRef]
34. Kulkarni-Narla A, Beitz AJ, Brown DR. 1999. Catecholaminergic, cholinergic and peptidergic innervation of gut-associated lymphoid tissue in porcine jejunum and ileum. *Cell Tissue Res* **298**: 275–286. [Medline] [CrossRef]
35. Lee WC, Bonin V, Reed M, Graham BJ, Hood G, Glattfelder K, Reid RC. 2016. Anatomy and function of an excitatory network in the visual cortex. *Nature* **532**: 370–374. [Medline] [CrossRef]
36. Li ZS, Furness JB. 1998. Immunohistochemical localisation of cholinergic markers in putative intrinsic primary afferent neurons of the guinea-pig small intestine. *Cell Tissue Res* **294**: 35–43. [Medline] [CrossRef]
37. Mantani Y, Haruta T, Nakanishi S, Sakata N, Yuasa H, Yokoyama T, Hoshi N. 2021. Ultrastructural and phenotypical diversity of macrophages in the rat ileal mucosa. *Cell Tissue Res* **385**: 697–711. [Medline] [CrossRef]
38. Mantani Y, Haruta T, Nishida M, Yokoyama T, Hoshi N, Kitagawa H. 2019. Three-dimensional analysis of fibroblast-like cells in the lamina propria of the rat ileum using serial block-face scanning electron microscopy. *J Vet Med Sci* **81**: 454–465. [Medline] [CrossRef]
39. Mantani Y, Yuasa H, Nishida M, Takahara E, Omotehara T, Udayanga KG, Kawano J, Yokoyama T, Hoshi N, Kitagawa H. 2014. Peculiar composition of epithelial cells in follicle-associated intestinal crypts of Peyer's patches in the rat small intestine. *J Vet Med Sci* **76**: 833–838. [Medline] [CrossRef]
40. Macrae IM, Furness JB, Costa M. 1986. Distribution of subgroups of noradrenaline neurons in the coeliac ganglion of the guinea-pig. *Cell Tissue Res* **244**: 173–180. [Medline] [CrossRef]
41. Matthews MR, Cuello AC. 1982. Substance P-immunoreactive peripheral branches of sensory neurons innervate guinea pig sympathetic neurons.

Proc Natl Acad Sci USA **79**: 1668–1672. [Medline] [CrossRef]
42. Mongardi Fantaguzzi C, Thacker M, Chiocchetti R, Furness JB. 2009. Identification of neuron types in the submucosal ganglia of the mouse ileum. *Cell Tissue Res* **336**: 179–189. [Medline] [CrossRef]
43. Morgan JL, Berger DR, Wetzel AW, Lichtman JW. 2016. The fuzzy logic of network connectivity in mouse visual thalamus. *Cell* **165**: 192–206. [Medline] [CrossRef]
44. Nagahama M, Semba R, Tsuzuki M, Ozaki T. 2001. Distribution of peripheral nerve terminals in the small and large intestine of congenital aganglionosis rats (Hirschsprung's disease rats). *Pathol Int* **51**: 145–157. [Medline] [CrossRef]
45. Nakanishi S, Mantani Y, Haruta T, Yokoyama T, Hoshi N. 2020. Three-dimensional analysis of neural connectivity with cells in rat ileal mucosa by serial block-face scanning electron microscopy. *J Vet Med Sci* **82**: 990–999. [Medline] [CrossRef]
46. Ohno N, Katoh M, Saitoh Y, Saitoh S, Ohno S. 2015. Three-dimensional volume imaging with electron microscopy toward connectome. *Microscopy (Oxf)* **64**: 17–26. [Medline] [CrossRef]
47. Ootani A, Li X, Sangiorgi E, Ho QT, Ueno H, Toda S, Sugihara H, Fujimoto K, Weissman IL, Capecchi MR, Kuo CJ. 2009. Sustained in vitro intestinal epithelial culture within a Wnt-dependent stem cell niche. *Nat Med* **15**: 701–706. [Medline] [CrossRef]
48. Qu ZD, Thacker M, Castelucci P, Bagyánszki M, Epstein ML, Furness JB. 2008. Immunohistochemical analysis of neuron types in the mouse small intestine. *Cell Tissue Res* **334**: 147–161. [Medline] [CrossRef]
49. Sang Q, Young HM. 1998. The identification and chemical coding of cholinergic neurons in the small and large intestine of the mouse. *Anat Rec* **251**: 185–199. [Medline] [CrossRef]
50. Sarna SK. 2008. Are interstitial cells of Cajal plurifunction cells in the gut? *Am J Physiol Gastrointest Liver Physiol* **294**: G372–G390. [Medline] [CrossRef]
51. Satoh Y. 1988. Atropine inhibits the degranulation of Paneth cells in ex-germ-free mice. *Cell Tissue Res* **253**: 397–402. [Medline] [CrossRef]
52. Stead RH, Tomioka M, Quinonez G, Simon GT, Felten SY, Bienenstock J. 1987. Intestinal mucosal mast cells in normal and nematode-infected rat intestines are in intimate contact with peptidergic nerves. *Proc Natl Acad Sci USA* **84**: 2975–2979. [Medline] [CrossRef]
53. Straub RH, Wiest R, Strauch UG, Härle P, Schölmerich J. 2006. The role of the sympathetic nervous system in intestinal inflammation. *Gut* **55**: 1640–1649. [Medline] [CrossRef]
54. Stzepourginski I, Nigro G, Jacob JM, Dulauroy S, Sansonetti PJ, Eberl G, Peduto L. 2017. CD34+ mesenchymal cells are a major component of the intestinal stem cells niche at homeostasis and after injury. *Proc Natl Acad Sci USA* **114**: E506–E513. [Medline] [CrossRef]
55. Tamura S, Mantani Y, Nakanishi S, Ohno N, Yokoyama T, Hoshi N. 2022. Region specificity of fibroblast-like cells in the mucosa of the rat large intestine. *Cell Tissue Res* **389**: 427–441. [Medline] [CrossRef]
56. Timmermans JP, Hens J, Adriaensen D. 2001. Outer submucous plexus: an intrinsic nerve network involved in both secretory and motility processes in the intestine of large mammals and humans. *Anat Rec* **262**: 71–78. [Medline] [CrossRef]
57. Wang FB, Powley TL. 2000. Topographic inventories of vagal afferents in gastrointestinal muscle. *J Comp Neurol* **421**: 302–324. [Medline] [CrossRef]
58. Weihe E, Tao-Cheng JH, Schäfer MK, Erickson JD, Eiden LE. 1996. Visualization of the vesicular acetylcholine transporter in cholinergic nerve terminals and its targeting to a specific population of small synaptic vesicles. *Proc Natl Acad Sci USA* **93**: 3547–3552. [Medline] [CrossRef]